

SCIENTIFIC REPORTS



OPEN

PERK Signaling Regulates Extracellular Proteostasis of an Amyloidogenic Protein During Endoplasmic Reticulum Stress

Received: 4 October 2018
 Accepted: 28 November 2018
 Published online: 23 January 2019

Isabelle C. Romine & R. Luke Wiseman 

The PERK arm of the unfolded protein response (UPR) regulates cellular proteostasis and survival in response to endoplasmic reticulum (ER) stress. However, the impact of PERK signaling on extracellular proteostasis is poorly understood. We define how PERK signaling influences extracellular proteostasis during ER stress using a conformational reporter of the secreted amyloidogenic protein transthyretin (TTR). We show that inhibiting PERK signaling impairs secretion of destabilized TTR during thapsigargin (Tg)-induced ER stress by increasing its ER retention in chaperone-bound complexes. Interestingly, PERK inhibition increases the ER stress-dependent secretion of TTR in non-native conformations that accumulate extracellularly as soluble oligomers. Pharmacologic or genetic TTR stabilization partially restores secretion of native TTR tetramers. However, PERK inhibition still increases the ER stress-dependent secretion of TTR in non-native conformations under these conditions, indicating that the conformation of stable secreted proteins can also be affected by inhibiting PERK. Our results define a role for PERK in regulating extracellular proteostasis during ER stress and indicate that genetic or aging-related alterations in PERK signaling can exacerbate ER stress-related imbalances in extracellular proteostasis implicated in diverse diseases.

The PERK signaling arm of the unfolded protein response (UPR) has a critical role in defining cellular survival in response to pathologic insults that disrupt endoplasmic reticulum (ER) proteostasis (i.e., ER stress). PERK is activated in response to ER stress through a mechanism involving PERK dimerization and autoprophosphorylation^{1,2}. Once activated, PERK phosphorylates the α subunit of eukaryotic initiation factor 2 (eIF2 α). This results in both a transient attenuation in new protein synthesis and the activation of stress-responsive transcription factors such as ATF4^{3–5}. PERK-dependent ATF4 activation induces expression of stress-responsive genes involved in diverse biologic functions including cellular redox, amino acid biosynthesis, and apoptotic signaling^{3,6,7}. Apart from eIF2 α , PERK also phosphorylates NRF2 to promote cellular redox regulation during ER stress^{8,9}. Through this integration of transcriptional and translational signaling, PERK has a central role in dictating cellular proteostasis and survival in response to varying levels of ER stress. During acute ER insults, PERK signaling is important for regulating protective biologic functions including metabolite homeostasis, cellular redox homeostasis and mitochondrial function^{8,10–12}. However, chronic PERK activation caused by severe or persistent ER stress promotes apoptotic signaling primarily through the PERK-dependent transcriptional regulation of pro-apoptotic factors^{13,14}.

Consistent with a role for PERK in dictating both protective and pro-apoptotic responses to specific ER insults, imbalances in PERK activity caused by genetic, environmental, or aging-related factors is implicated in the pathogenesis of diverse diseases. Sustained PERK signaling associated with chronic or severe ER insults is implicated in neurodegeneration associated with diseases such as Alzheimer's disease and prion disease^{15,16}. As such, pharmacologic inhibition of PERK has emerged as a potential strategy to ameliorate neurodegeneration-associated pathologies involved in these disorders¹⁵. In contrast, genetic and pharmacologic evidence demonstrates that reductions in PERK signaling also influence disease pathogenesis. Loss-of-function mutations in *PERK* promote neonatal diabetes in mouse models and the human disease Wolcott-Rallison syndrome^{17,18}. Similarly, hypomorphic *PERK* alleles are implicated in the tau-associated neurodegenerative disorder progressive supranuclear palsy

Department of Molecular Medicine, The Scripps Research Institute, La Jolla, CA, 92037, USA. Correspondence and requests for materials should be addressed to R.L.W. (email: wiseman@scripps.edu)

(PSP), suggesting that reduced PERK signaling promotes toxic tau aggregation^{19,20}. Consistent with this, pharmacologic PERK activation attenuates aggregation and toxicity of PSP-related tau mutants in mouse models²¹. Pharmacologic or chemical genetic increases in PERK signaling also reduce the toxic aggregation of rhodopsin mutants associated with retinal degeneration^{19,22,23}. Thus, while significant focus has been directed to the pathologic importance of overactive or chronic PERK signaling in disease, it is clear that deficiencies in PERK activity also promote pathogenesis, reflecting a protective role for this UPR signaling arm in regulating cellular physiology in response to ER stress.

Interestingly, recent work has revealed PERK as a critical regulator of proteostasis within the ER – the first organelle of the secretory pathway. PERK-dependent translation attenuation regulates ER protein folding load in response to acute ER stress, freeing ER proteostasis factors to protect the secretory proteome from misfolding during the initial stages of toxic insult^{2,24}. In addition, PERK regulates both ER-to-Golgi anterograde trafficking and ER-associated degradation^{25,26}, the latter a primary mechanism by which cells degrade ER proteins²⁷. As such, genetic or pharmacologic inhibition of PERK signaling disrupts secretory proteostasis to reduce the secretion and increase the intracellular accumulation of proteins such as collagen, insulin, or mutant rhodopsin as high molecular weight (HMW) aggregates^{28–31}. These results define an important role for PERK in regulating ER proteostasis in response to pathologic insults. However, considering the importance of the ER in regulating proteostasis in downstream secretory environments such as the extracellular space, a critical question remains: “How does PERK signaling impact extracellular proteostasis in response to ER stress?”

Imbalances in ER proteostasis can propagate to extracellular environments through the secretion of proteins in non-native conformations that accumulate as toxic oligomers and aggregates associated with proteotoxicity in etiologically-diverse protein aggregation diseases, including many amyloid diseases^{32–34}. Thus, impaired secretory proteostasis afforded by genetic or aging-related imbalances in PERK activity could exacerbate ER stress-dependent increases in the secretion of non-native proteins, challenging the conformational integrity of the secreted proteome and increasing extracellular populations of toxic oligomers. Here, we use a conformational reporter of the model secreted amyloidogenic protein transthyretin (TTR) – a natively tetrameric protein that aggregates into toxic oligomers and amyloid fibrils associated with diverse TTR-related amyloid diseases^{35,36} – to define how pharmacologic inhibition of PERK signaling impacts extracellular proteostasis in response to ER stress. We show that co-administration of PERK inhibitors and ER stress induced by the SERCA inhibitor thapsigargin (Tg) increases secretion of destabilized and wild-type TTR in non-native conformations that accumulate extracellularly as soluble oligomers, the TTR conformation commonly associated with proteotoxicity in disease³⁵. These results demonstrate that alterations in PERK signaling can challenge extracellular proteostasis by reducing the secretion of proteins in native, functional conformations and increasing the extracellular accumulation of soluble oligomers associated with the pathogenesis of diverse protein aggregation diseases.

Results and Discussion

Pretreatment with Tg and PERK inhibitors disrupts secretion of destabilized $^{FT}TTR^{A25T}$. Previously, we showed that administration of Tg reduces the secretion of destabilized, aggregation-prone TTR variants such as TTR^{A25T} ^{33,37,38}. To define how PERK inhibition influences the Tg-dependent reduction in TTR^{A25T} secretion, we pretreated HEK293T cells expressing FLAG-tagged TTR^{A25T} ($^{FT}TTR^{A25T}$) with Tg and/or the PERK signaling inhibitor ISRib for 16 h and then monitored $^{FT}TTR^{A25T}$ secretion by [³⁵S] metabolic labeling (Fig. 1A). ISRib is an antagonist of PERK signaling that binds to eIF2B and desensitizes cells to eIF2 α phosphorylation^{39,40}. Importantly, co-pretreatment with Tg and ISRib increased metabolic labeling of $^{FT}TTR^{A25T}$ relative to pretreatment with Tg alone (Fig. 1A,B). This is consistent with ISRib blocking Tg-dependent translational attenuation downstream of PERK^{39,40}. Interestingly, co-pretreatment with ISRib and Tg enhanced the Tg-dependent reduction in the fraction of $^{FT}TTR^{A25T}$ secreted (Fig. 1A,C). The enhanced reduction in $^{FT}TTR^{A25T}$ fraction secretion observed upon Tg and ISRib co-pretreatment did not correspond with an increased loss of total $^{FT}TTR^{A25T}$, indicating that this condition does not increase $^{FT}TTR^{A25T}$ degradation (Fig. 1A,D). Instead, this pretreatment increased the accumulation of $^{FT}TTR^{A25T}$ in lysate fractions, reflecting increased intracellular retention (Fig. 1A,E). Interestingly, while the fraction of $^{FT}TTR^{A25T}$ secreted to the media is reduced in cells co-pretreated with Tg and ISRib relative to pretreatment with Tg alone, the total amount of [³⁵S]-labeled $^{FT}TTR^{A25T}$ that accumulates in media is similar between these conditions, albeit lower than that observed in controls (Fig. S1A). This reflects the higher expression of $^{FT}TTR^{A25T}$ observed in cells co-pretreated with Tg and ISRib (Fig. 1B). Identical results were obtained using the PERK inhibitor GSK2656157 (herein referred to as GSK), which blocks PERK signaling through direct binding to the PERK kinase active site (Fig. S1A–E)⁴¹. The use of the two mechanistically distinct inhibitors of PERK signaling indicates that the enhanced reduction in $^{FT}TTR^{A25T}$ secretion observed in cells co-pretreated with Tg and PERK inhibitors cannot be attributed to off-pathway activities of these compounds⁴². Thus, these results show that pharmacologic inhibition of PERK signaling impairs secretory proteostasis of $^{FT}TTR^{A25T}$ during ER stress.

PERK inhibition increases Tg-dependent interactions between $^{FT}TTR^{A25T}$ and ER chaperones. The intracellular retention of $^{FT}TTR^{A25T}$ observed upon co-pretreatment with Tg and ISRib likely reflects increased accumulation of non-native TTR conformations within the ER, as observed for other proteins^{28,29,31}. To test this, we measured the intracellular interaction between $^{FT}TTR^{A25T}$ and ER chaperones (which bind non-native protein conformations) in HEK293T cells pretreated with Tg and/or ISRib for 16 h using an established immunopurification (IP)/immunoblotting (IB) assay³⁸. Pretreatment with Tg increases the relative recovery of the ER ATP-dependent HSP70 chaperone BiP and the BiP co-chaperones ERdj3 and HYOU1 in $^{FT}TTR^{A25T}$ IPs (Figs 1F and S1F). This indicates that Tg pretreatment increases the non-native population of intracellular TTR that can engage ER chaperones. Co-pretreatment with Tg and ISRib further increased the relative interactions between $^{FT}TTR^{A25T}$ and these ER chaperones, as compared to Tg pretreatment alone. Importantly, we

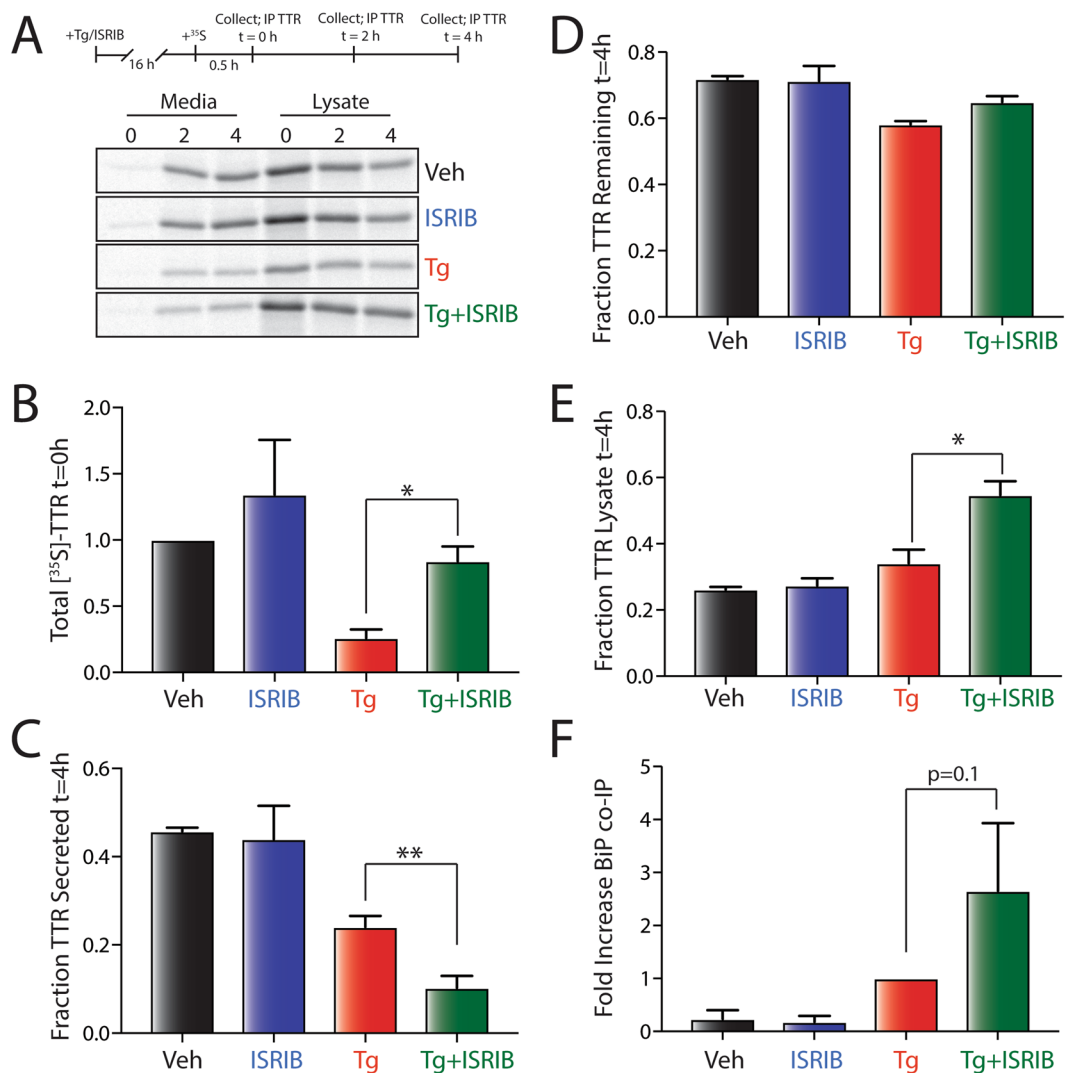


Figure 1. Pharmacologic inhibition of PERK signaling disrupts ^{35}S -labeled $\text{FTTTR}^{\text{A}25\text{T}}$ secretory proteostasis during Tg-induced ER stress. (A) Representative autoradiogram of ^{35}S -labeled $\text{FTTTR}^{\text{A}25\text{T}}$ in lysates and media collected from HEK293T cells pretreated for 16 h with thapsigargin (Tg; 500 nM) and/or ISRB (200 nM). The protocol for the experiment is shown above. (B) Graph showing the total amount of ^{35}S -labeled $\text{FTTTR}^{\text{A}25\text{T}}$ at $t = 0\text{ h}$ in HEK293T cells pretreated for 16 h with thapsigargin (Tg; 500 nM) and/or ISRB (200 nM). Data are shown normalized to vehicle-treated cells. Error bars show SEM for $n = 3$ independent experiments. A representative autoradiogram is shown in (A). (C) Graph showing the fraction ^{35}S -labeled $\text{FTTTR}^{\text{A}25\text{T}}$ secreted at $t = 4\text{ h}$ in HEK293T cells pretreated for 16 h with thapsigargin (Tg; 500 nM) and/or ISRB (200 nM). Fraction secreted was calculated as described in Materials and Methods. Error bars show SEM for $n = 3$ independent experiments. A representative autoradiogram is shown in (A). (D) Graph showing the fraction ^{35}S -labeled $\text{FTTTR}^{\text{A}25\text{T}}$ remaining at $t = 4\text{ h}$ in HEK293T cells pretreated for 16 h with thapsigargin (Tg; 500 nM) and/or ISRB (200 nM). Fraction remaining was calculated as described in Materials and Methods. Error bars show SEM for $n = 3$ independent experiments. A representative autoradiogram is shown in (A). (E) Graph showing the fraction ^{35}S -labeled $\text{FTTTR}^{\text{A}25\text{T}}$ in lysates at $t = 4\text{ h}$ in HEK293T cells pretreated for 16 h with thapsigargin (Tg; 500 nM) and/or ISRB (200 nM). Fraction lysate was calculated as described in Materials and Methods. Error bars show SEM for $n = 3$ independent experiments. A representative autoradiogram is shown in (A). (F) Graph showing the recovery of BiP in anti-FLAG IPs from HEK293T cells expressing $\text{FTTTR}^{\text{A}25\text{T}}$ and pretreated for 16 h with Tg (500 nM) and/or ISRB (200 nM). Data are shown normalized to Tg-treated cells. Error bars show SEM for $n = 3$ independent experiments. A representative immunoblot is shown in Fig. S1F. *Indicates $p < 0.05$; ** indicates $p < 0.01$ for a paired two-tailed t-test.

do not observe statistically significant differences in the intracellular levels of BiP or HYOU1 in cells pretreated with Tg versus cells co-pretreated with Tg and ISRB (Fig. S1F–I). This indicates that ISRB-dependent inhibition of PERK signaling does not globally disrupt ER stress-dependent upregulation of these UPR target genes. Instead, this result suggests that disruption of $\text{FTTTR}^{\text{A}25\text{T}}$ secretion afforded by PERK inhibition likely results from impaired translational attenuation. However, we cannot rule out the possibility that altered transcription of other ER stress-regulated proteins contribute to the altered secretion of $\text{FTTTR}^{\text{A}25\text{T}}$ observed in cells co-treated

with Tg and ISRB. Collectively, these results indicate that the increased accumulation of destabilized $^{FT}TTR^{A25T}$ afforded by co-pretreatment with PERK inhibitors and Tg reflects increased ER retention of non-native TTR in chaperone-bound complexes. This suggests that PERK inhibition during ER stress disrupts the ability of cells to properly fold and assemble $^{FT}TTR^{A25T}$ into its native tetrameric conformation.

PERK inhibition reduces the population of $^{FT}TTR^{A25T}$ secreted as native tetramers during Tg-induced ER stress. Imbalances in ER proteostasis can propagate to extracellular environments through the secretion of proteins in non-native conformations^{32,33}. Thus, we used a previously established assay to define how co-treatment with PERK inhibitors and Tg-induced ER stress impacts the conformation of $^{FT}TTR^{A25T}$ secreted from mammalian cells (Fig. 2A)³³. In this assay, we collect conditioned media for 16 h on cells expressing $^{FT}TTR^{A25T}$ prepared in the presence of the cell impermeable compound tafamidis-sulfonate (Taf-S; Fig. S2A) – a compound that immediately binds and stabilizes native TTR tetramers once secreted to the extracellular space³³. We then quantify total, tetrameric, and aggregate TTR in this conditioned media. Total TTR is quantified by SDS-PAGE/IB. Tetrameric TTR is measured by incubating conditioned media with compound 1 (Fig. S2A) – a fluorogenic compound that readily displaces the Taf-S in the two small-molecule binding sites of the native TTR tetramer and becomes fluorescent upon binding^{33,43,44}. Tetramers are then separated by anion exchange chromatography and quantified by compound 1 fluorescence (Fig. S2A). Finally, soluble TTR aggregates are monitored by Clear Native (CN)-PAGE/IB^{33,34}. We previously used this approach to show that Tg treatment reduces the secretion of destabilized $^{FT}TTR^{A25T}$ as native tetramers and increases accumulation of this destabilized, aggregation-prone protein as soluble oligomers in conditioned media³³.

To define how PERK inhibition influences ER stress-dependent alterations in the conformation of secreted $^{FT}TTR^{A25T}$, we conditioned media in the presence of Taf-S for 16 h on HEK293T cells expressing $^{FT}TTR^{A25T}$ and treated with Tg and/or ISRB. We then measured total, tetrameric, and aggregate TTR using the assays described above (Fig. 2A). Treatment with Tg reduced the accumulation of total $^{FT}TTR^{A25T}$ in conditioned media, consistent with published results (Fig. 2B)^{33,38}. Surprisingly, co-treatment with ISRB rescued the Tg-dependent reduction in total $^{FT}TTR^{A25T}$ in conditioned media (Fig. 2B), likely reflecting the inhibition of PERK-regulated translational attenuation afforded by ISRB over the duration of the media conditioning (Fig. 1B). Interestingly, these results are distinct from those observed using [³⁵S] metabolic labeling, where we show that co-pretreatment with Tg and ISRB significantly impaired $^{FT}TTR^{A25T}$ secretion (see Figs 1C and S1A). This likely reflects differences in ER proteostasis afforded by the distinct experimental setups. In the SDS-PAGE experiment, the accumulation of TTR in conditioned media is monitored *during* a 16 h treatment where the ER proteostasis environment is in the process of changing due to both the ER stress and UPR activation. In contrast, the [³⁵S] metabolic labeling experiments measure $^{FT}TTR^{A25T}$ secretion *following* a 16 h pretreatment *after* the ER environment has been significantly altered. The fact that PERK inhibition influences TTR secretion under both paradigms highlights the dynamic impact ER stress has on ER function and underscores the critical role for PERK signaling in regulating TTR secretion in response to ER stress.

In order to define how PERK inhibition influences the conformation of $^{FT}TTR^{A25T}$ secreted during Tg-induced ER stress, we measured tetrameric $^{FT}TTR^{A25T}$ using our compound 1 fluorescence/anion exchange chromatography assay (Fig. 2A) in conditioned media prepared on cells co-treated with Tg and/or ISRB (the same media used to monitor total $^{FT}TTR^{A25T}$ levels in Fig. 2B). As reported previously³³, $^{FT}TTR^{A25T}$ tetramers in conditioned media migrate as multiple peaks by anion exchange chromatography, reflecting the distribution of heterotetramers consisting of unmodified subunits and subunits containing posttranslational modifications such as sulfenylation and cysteinylation (Fig. 2C). Co-treatment with Tg and ISRB significantly altered the distribution of these peaks, resulting in an increase of heterotetramers eluting earlier on the anion exchange column (Fig. 2C, green). This suggests that Tg and ISRB co-treatment alters posttranslational modifications of $^{FT}TTR^{A25T}$ secreted to the extracellular space. As expected, liquid chromatography (LC)-mass spectrometry (MS) analysis of $^{FT}TTR^{A25T}$ IP'd from conditioned media prepared on cells co-treated with Tg and ISRB shows increased relative populations of unmodified $^{FT}TTR^{A25T}$ (Fig. S2A). This is consistent with the earlier migration of tetramers observed under these conditions by anion exchange chromatography and demonstrates that PERK inhibition disrupts the secretory proteostasis environment to influence posttranslational TTR modifications during ER stress.

To quantify the recovery of $^{FT}TTR^{A25T}$ tetramers in conditioned media, we integrated the fluorescence across all of the tetramer peaks. We observed significant reductions in the recovery of $^{FT}TTR^{A25T}$ tetramers in media prepared on Tg-treated cells (Fig. 2B), consistent with published results³³. However, despite lower levels of total $^{FT}TTR^{A25T}$ in media conditioned on cells treated with Tg relative to cells treated with Tg and ISRB, identical amounts of tetramers were detected in conditioned media prepared under these two conditions (Fig. 2B). This indicates that PERK inhibition decreases the relative population of $^{FT}TTR^{A25T}$ secreted as native tetramers. This can be demonstrated by normalizing the recovered $^{FT}TTR^{A25T}$ tetramers by the total amount of $^{FT}TTR^{A25T}$ in media prepared on cells treated with Tg and/or ISRB³³. This normalization confirms that PERK inhibition reduces the population of $^{FT}TTR^{A25T}$ secreted as native tetramers during ER stress (Fig. 2D). Thus, our results show that PERK inhibition increases the ER-stress-dependent secretion of $^{FT}TTR^{A25T}$ in non-native conformations.

Inhibiting PERK during Tg-induced ER stress increases accumulation of extracellular $^{FT}TTR^{A25T}$ oligomers. Non-native $^{FT}TTR^{A25T}$ accumulates as soluble oligomers in conditioned media owing to the low stability of the aggregation-prone $^{FT}TTR^{A25T}$ variant^{33,34}. Thus, the increased *total* (Fig. 2B) and *non-native* (Fig. 2D) TTR in media conditioned on cells co-treated with Tg and ISRB should be reflected by increased accumulation of extracellular soluble oligomers in media prepared under these conditions. Tg treatment alone increased the accumulation of soluble $^{FT}TTR^{A25T}$ aggregates (Fig. 2E,F). This is consistent with previous results and further demonstrates the ER stress-dependent increase in the secretion of non-native $^{FT}TTR^{A25T}$ ³³. Interestingly, co-treatment with Tg and ISRB significantly increased $^{FT}TTR^{A25T}$ soluble aggregates in conditioned

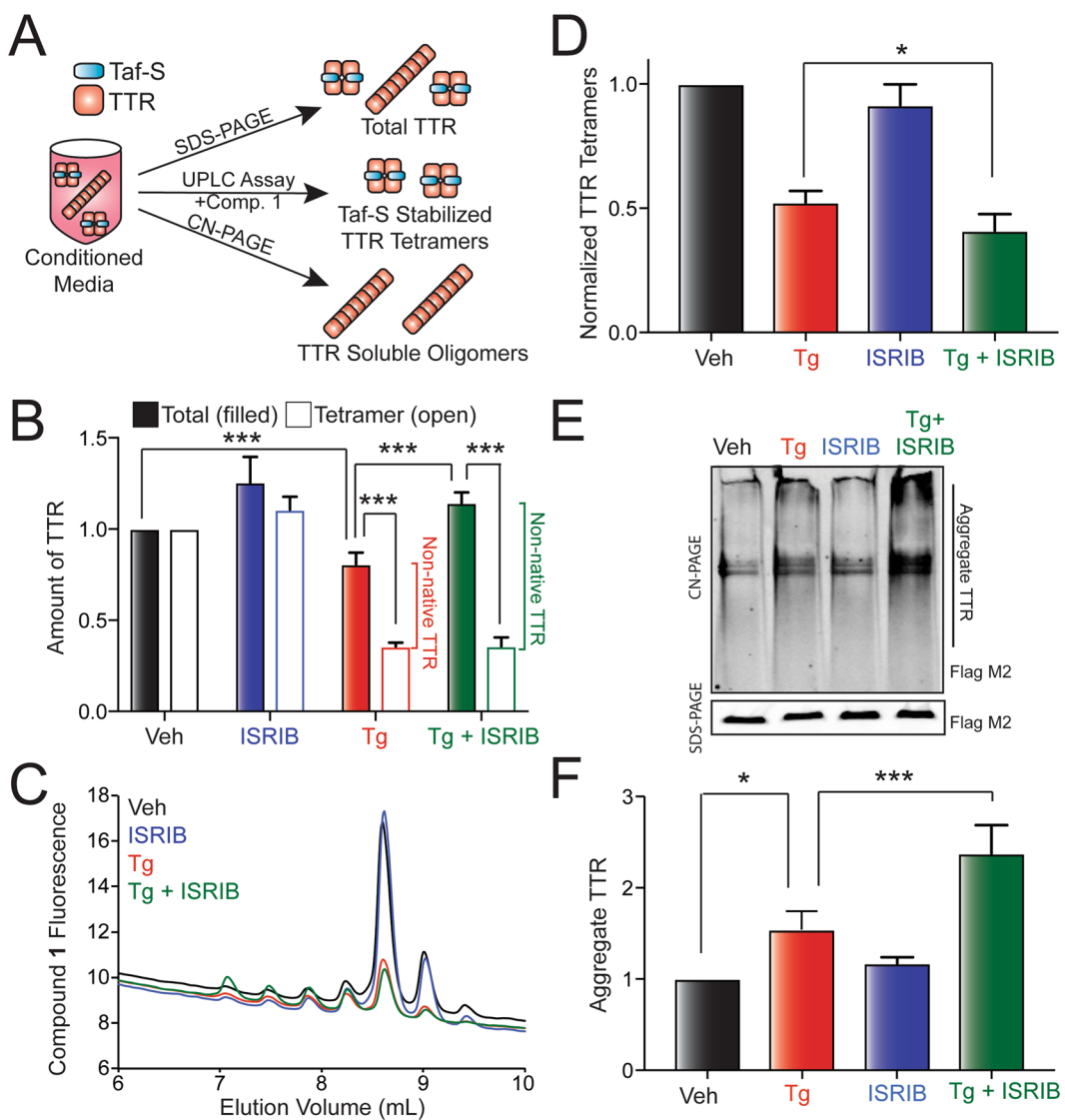


Figure 2. Pharmacologic inhibition of PERK signaling increases secretion of $^{FT}\text{TTR}^{\text{A}25\text{T}}$ in non-native conformations. (A) Illustration showing the three assays used to monitor total, tetrameric, and aggregate TTR in conditioned media. (B) Graph showing total (filled bars) and tetrameric (open bars) $^{FT}\text{TTR}^{\text{A}25\text{T}}$ in conditioned media prepared in the presence of Taf-S on HEK293T cells treated for 16 h with Tg (500 nM) and/or ISRB (200 nM). Total and tetrameric $^{FT}\text{TTR}^{\text{A}25\text{T}}$ are normalized to vehicle. Relative populations of non-native TTR in each condition are shown. Error bars show SEM for n = 13 independent experiments. (C) Representative chromatogram showing $^{FT}\text{TTR}^{\text{A}25\text{T}}$ tetramers in conditioned media prepared in the presence of Taf-S on HEK293T cells treated for 16 h with Tg (500 nM) and/or ISRB (200 nM). $^{FT}\text{TTR}^{\text{A}25\text{T}}$ tetramers were separated on anion exchange chromatography using the UPLC system and visualized by compound 1 fluorescence. (D) Graph showing normalized $^{FT}\text{TTR}^{\text{A}25\text{T}}$ tetramers in conditioned media prepared in the presence of Taf-S on HEK293T cells treated for 16 h with Tg (500 nM) and/or ISRB (200 nM). Normalized TTR tetramers were calculated using the formula: normalized TTR tetramers for a given condition = (TTR tetramer signal condition/TTR tetramer signal veh)/(total TTR signal condition/TTR tetramer signal veh). Error bars show SEM for n = 13 independent experiments. (E) Representative Clear Native (CN)-PAGE immunoblot of $^{FT}\text{TTR}^{\text{A}25\text{T}}$ soluble aggregates in conditioned media prepared in the presence of Taf-S on HEK293T cells treated for 16 h with Tg (500 nM) and/or ISRB (200 nM). Total $^{FT}\text{TTR}^{\text{A}25\text{T}}$ in each condition is shown in the SDS-PAGE immunoblot. (F) Graph showing the amounts of $^{FT}\text{TTR}^{\text{A}25\text{T}}$ soluble aggregates in conditioned media prepared in the presence of Taf-S on HEK293T cells treated for 16 h with Tg (500 nM) and/or ISRB (200 nM). Aggregate $^{FT}\text{TTR}^{\text{A}25\text{T}}$ is normalized to vehicle. Error bars show SEM for n = 13 independent experiments. *Indicates p < 0.05, *** indicates p < 0.005 for a two-tailed paired t-test.

media relative to treatment with Tg alone (Fig. 2E,F), consistent with the increase in non-native $^{FT}\text{TTR}^{\text{A}25\text{T}}$ secreted under these conditions (Fig. 2B,D). These results demonstrate that inhibiting PERK signaling during Tg-induced ER stress disrupts extracellular proteostasis by exacerbating the Tg-dependent secretion of destabilized $^{FT}\text{TTR}^{\text{A}25\text{T}}$ in non-native conformations that accumulate extracellularly as soluble oligomers.

Pharmacologic stabilization of TTR tetramers partially rescues the secretion of native $\text{FTTTR}^{\text{A25T}}$ tetramers in cells treated with Tg and PERK inhibitors. TTR tetramers can be stabilized intracellularly by administration of the cell permeable kinetic stabilizer tafamidis (Taf)^{33,37}. Taf-dependent intracellular stabilization prevents the dissociation of tetramers prior to secretion to the extracellular space. Thus, conditioning media in the presence of Taf provides an opportunity to determine whether the increased populations of $\text{FTTTR}^{\text{A25T}}$ secreted from cells co-treated with Tg and ISRB reflects increased dissociation of tetramers during the secretion process (i.e., reduced tetramer stability) and/or increased secretion of $\text{FTTTR}^{\text{A25T}}$ prior to tetramer assembly (i.e., reduced tetramer assembly). To test this, we conditioned media on HEK293T cells expressing $\text{FTTTR}^{\text{A25T}}$ treated with Tg and/or ISRB in the presence of either Taf-S or Taf. We then monitored total, tetrameric, and aggregate TTR using the assays shown in Fig. 2A.

Conditioning media in the presence of Taf significantly increased the recovery of $\text{FTTTR}^{\text{A25T}}$ tetramers in every condition, relative to media conditioned in the presence of Taf-S (Figs 3A,B and S3). This indicates that Taf-dependent intracellular stabilization of $\text{FTTTR}^{\text{A25T}}$ tetramers increases secretion of $\text{FTTTR}^{\text{A25T}}$ as native tetramers. This increase cannot be attributed to alterations in $\text{FTTTR}^{\text{A25T}}$ posttranslational modifications, as the addition of Taf does not alter the shift in tetramer distribution observed in cells co-treated with Tg and ISRB (Fig. 3B). Importantly, the increased secretion of $\text{FTTTR}^{\text{A25T}}$ tetramers corresponds with reductions of soluble $\text{FTTTR}^{\text{A25T}}$ aggregates in conditioned media (Fig. 3C). This demonstrates that Taf-dependent intracellular stabilization of TTR reduces the secretion of $\text{FTTTR}^{\text{A25T}}$ in non-native conformations under all conditions. This also indicates that the accumulation of non-native TTR observed in media conditioned in the presence of Taf-S partially reflects dissociation of TTR tetramers (that can be stabilized intracellularly by Taf) within the secretory pathway. This reveals a specific advantage for employing kinetic stabilizing compounds such as Taf that are cell permeable, as these compounds can stabilize aggregation-prone proteins intracellularly and mitigate potential imbalances in secretory proteostasis associated with the aberrant secretion of non-native conformations.

Despite the increased secretion of $\text{FTTTR}^{\text{A25T}}$ tetramers afforded by Taf-dependent intracellular stabilization, in the presence of Taf, co-administration of Tg and ISRB still increased secretion of $\text{FTTTR}^{\text{A25T}}$ in non-native conformations, relative to Tg treatment alone (Fig. 3A,D). Consistent with this, conditioned media prepared on cells co-treated with Tg and ISRB in the presence of Taf show higher levels of soluble $\text{FTTTR}^{\text{A25T}}$ oligomers relative to Tg-treated cells, albeit significantly less than that observed for media conditioned in the presence of Taf-S (Fig. 3C). This demonstrates that despite the ability for Taf to stabilize a large population of $\text{FTTTR}^{\text{A25T}}$ tetramers in the secretory environment, PERK inhibition can still increase the secretion of $\text{FTTTR}^{\text{A25T}}$ in non-native conformations during Tg-induced ER stress.

Secretion of stable, wild-type TTR as native tetramers is reduced in cells co-treated with Tg and PERK inhibition. The ability for PERK inhibition to promote Tg-dependent secretion of $\text{FTTTR}^{\text{A25T}}$ in non-native conformations even in the presence of the stabilizing ligand Taf suggests that stable, wild-type TTR (TTR^{WT}) could similarly be susceptible to reductions in tetramer secretion under these conditions. Initially, we confirmed that PERK inhibition disrupts secretory proteostasis for stable FTTTR^{WT} by monitoring the interactions between FTTTR^{WT} and ER chaperones in HEK293T cells treated with Tg and/or the PERK inhibitor GSK. Co-treatment with Tg and GSK significantly increased relative interactions between FTTTR^{WT} and the ER chaperones BiP, ERdj3, and HYOU1 (Fig. 4A), mimicking the results observed with destabilized $\text{FTTTR}^{\text{A25T}}$ (Figs 1F and S1F). Furthermore, co-treatment with Tg and GSK increased intracellular levels of FTTTR^{WT} , suggesting that this condition leads to intracellular accumulation of stable FTTTR^{WT} (Fig. S4A). However, we did not observe significant increases in intracellular levels of BiP or HYOU1, further demonstrating that PERK inhibition does not impact Tg-dependent increases in these chaperones (Fig. S1G–I and S4A). Collectively, these results indicate that PERK inhibition during ER stress disrupts secretory proteostasis of stable, wild-type TTR by increasing its ER retention in chaperone-bound complexes – results analogous to that observed for destabilized $\text{FTTTR}^{\text{A25T}}$ (Figs 1F and S1F).

Next, we conditioned media in the presence of Taf-S on HEK293T cells expressing FTTTR^{WT} treated with Tg and/or GSK and monitored the recovery of total, tetrameric, or aggregate TTR using the assays described in Fig. 2A. Tg and GSK co-treatment increased the population of FTTTR^{WT} secreted in non-native conformations (Figs 4B,C and S4A). Identical results were observed in cells co-treated with Tg and ISRB (Fig. 4D,E). Normalizing the recovered FTTTR^{WT} tetramers by the total amount of FTTTR^{WT} in conditioned media confirms that PERK inhibition reduces the population of stable FTTTR^{WT} secreted as tetramers during ER stress (Fig. 4F). Unfortunately, the stability of FTTTR^{WT} monomers (relative to $\text{FTTTR}^{\text{A25T}}$ monomers) combined with the relatively low concentrations of non-native FTTTR^{WT} in conditioned media hinders the aggregation of this protein in the extracellular space, making it difficult to reproducibly visualize FTTTR^{WT} soluble aggregates in conditioned media⁴⁵. However, co-treatment with Tg and GSK does appear to increase the population of FTTTR^{WT} soluble aggregates observed by CN-PAGE/IB, consistent with the increased secretion of this protein in non-native conformations (Fig. S4C). Collectively, these results show that PERK inhibition increases the Tg-dependent secretion of wild-type TTR in non-native conformations, indicating that PERK inhibition can disrupt extracellular proteostasis of stable secreted proteins during Tg-induced ER stress.

Concluding Remarks

Imbalances in PERK signaling are implicated in the onset and pathogenesis of etiologically-diverse diseases^{15–23}. Here, we show that PERK inhibition during Tg-induced ER stress increases the secretion of the disease relevant amyloidogenic protein TTR in non-native conformations that accumulate extracellularly as soluble oligomers. This indicates that PERK signaling has an important role in dictating extracellular proteostasis by controlling the conformational integrity of secreted proteins such as TTR. As such, genetic, aging-related, or pharmacologic conditions that reduce PERK signaling could lead to pathologic imbalances in extracellular proteostasis that contribute to human disease. The increased secretion of proteins in non-native conformations would

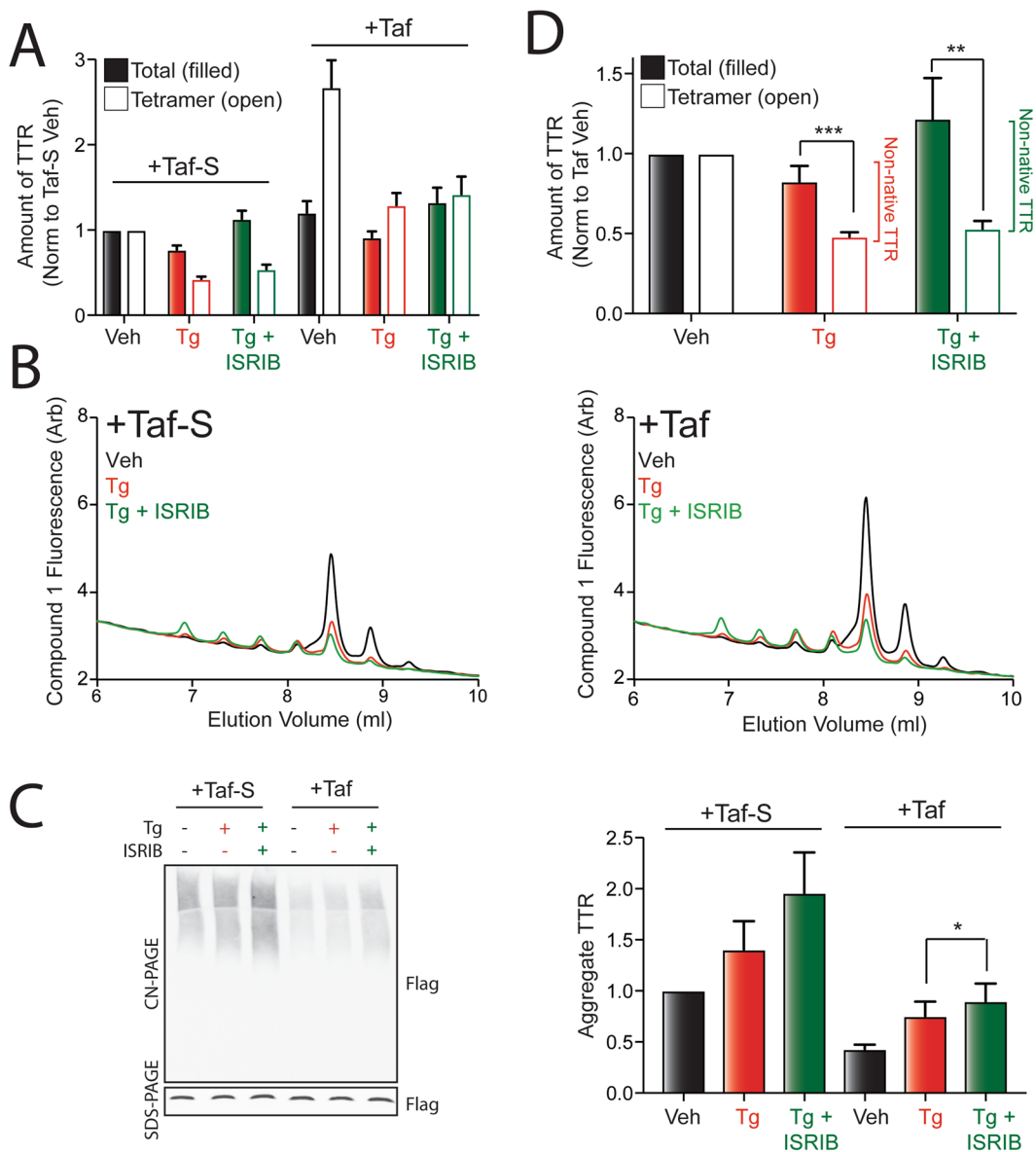


Figure 3. Pharmacologic stabilization of $^{FT}\text{TTR}^{\text{A}25\text{T}}$ tetramers partially restores secretion in native conformations. (A) Graph showing total (filled bars) and tetrameric (open bars) $^{FT}\text{TTR}^{\text{A}25\text{T}}$ in conditioned media prepared in the presence of Taf-S or Taf on HEK293T cells treated for 16 h with Tg (500 nM) and/or ISRIB (200 nM). Total and tetrameric $^{FT}\text{TTR}^{\text{A}25\text{T}}$ are normalized to media prepared on vehicle-treated cells in the presence of Taf-S. Error bars show SEM for $n = 8$ independent experiments. (B) Representative chromatogram showing $^{FT}\text{TTR}^{\text{A}25\text{T}}$ tetramers in conditioned media prepared in the presence of Taf-S (left) or Taf (right) on HEK293T cells treated for 16 h with Tg (500 nM) and/or ISRIB (200 nM). $^{FT}\text{TTR}^{\text{A}25\text{T}}$ tetramers were separated on anion exchange chromatography using the UPLC system and visualized by compound 1 fluorescence. (C) Representative CN-PAGE/immunoblot (left) and quantification (right) of $^{FT}\text{TTR}^{\text{A}25\text{T}}$ aggregates in conditioned media prepared in the presence of Taf-S or Taf on HEK293T cells treated for 16 h with Tg (500 nM) and/or ISRIB (200 nM). Total $^{FT}\text{TTR}^{\text{A}25\text{T}}$ in each condition is shown in the SDS-PAGE immunoblot. Error bars show SEM for $n = 5$ independent experiments. (D) Graph showing total (filled bars) and tetrameric (open bars) $^{FT}\text{TTR}^{\text{A}25\text{T}}$ in conditioned media prepared in the presence of Taf-S or Taf on HEK293T cells treated for 16 h with Tg (500 nM) and/or ISRIB (200 nM). Total and tetrameric $^{FT}\text{TTR}^{\text{A}25\text{T}}$ are normalized to media prepared on vehicle-treated cells in the presence of Taf. Relative populations of non-native TTR in each condition are shown. Error bars show SEM for $n = 8$ independent experiments. *Indicates $p < 0.05$, ** $p < 0.01$, and *** $p < 0.005$ for a two-tailed paired t-test.

increase extracellular populations available for concentration-dependent aggregation into toxic oligomers and amyloid fibrils, as we show for TTR. Alternatively, reduced secretion of proteins in native conformations could also prevent important functions of secreted proteins in biologic activities such as hormonal signaling, cell-cell

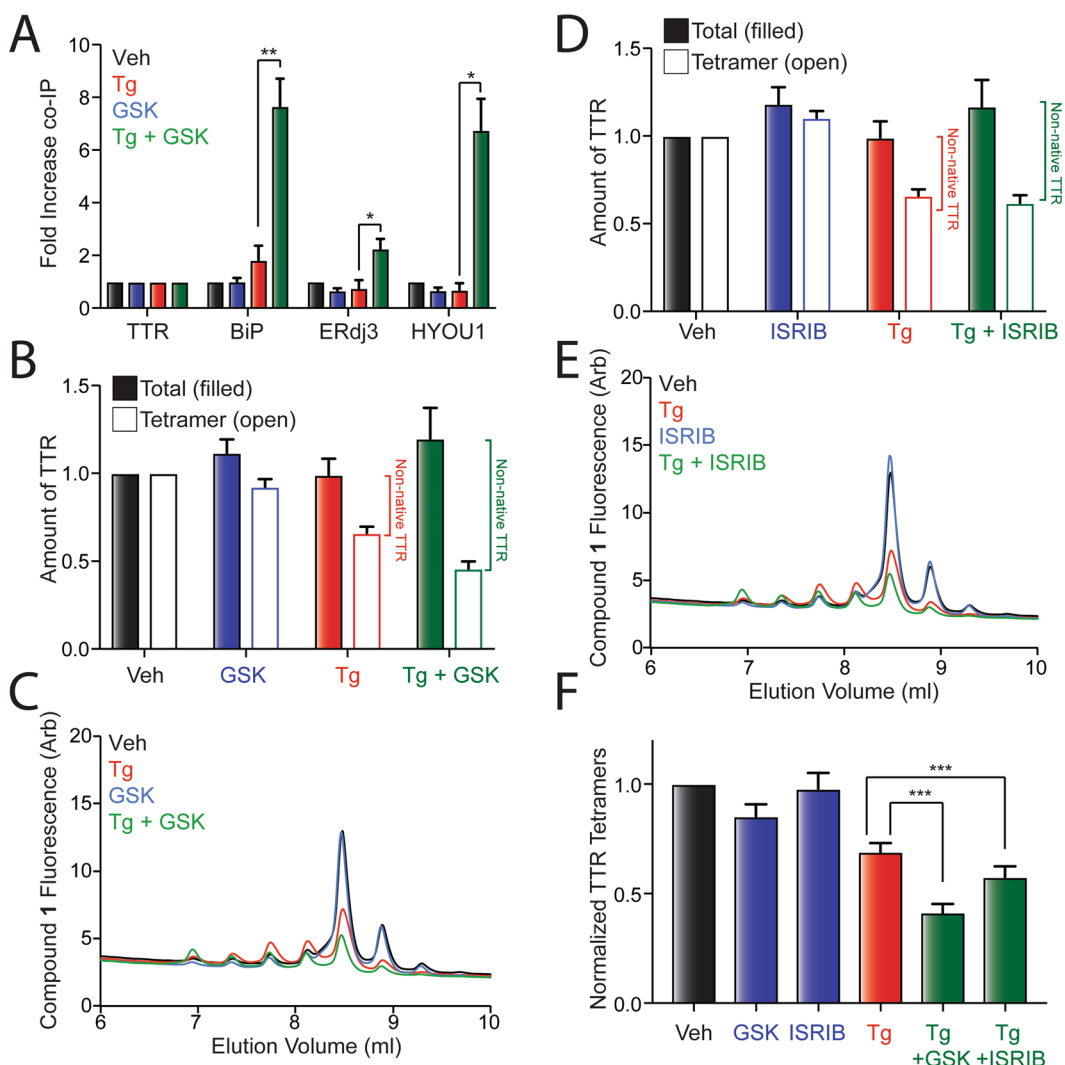


Figure 4. PERK inhibition increases secretion of stable, wild-type TTR in non-native conformations during Tg-induced ER stress. (A) Graph showing the recovery of TTR, BiP, ERdj3, and HYOU1 in anti-FLAG IPs from HEK293T cells expressing $^{FT}TTR^{WT}$ and pretreated for 16 h with Tg (500 nM) and/or GSK (300 nM). Error bars show SEM for $n = 4$ independent experiments. A representative immunoblot is shown in Fig. S4A. (B) Graph showing total (filled bars) and tetrameric (open bars) $^{FT}TTR^{WT}$ in conditioned media prepared in the presence of Taf-S on HEK293T cells treated for 16 h with Tg (500 nM) and/or GSK (300 nM). Total and tetrameric $^{FT}TTR^{WT}$ are normalized to media prepared on vehicle-treated cells. Relative populations of non-native TTR in each condition are shown. Error bars show SEM for $n = 10$ independent experiments. (C) Representative chromatogram showing $^{FT}TTR^{WT}$ tetramers in conditioned media prepared in the presence of Taf-S on HEK293T cells treated for 16 h with Tg (500 nM) and/or GSK (300 nM). $^{FT}TTR^{WT}$ tetramers were separated on anion exchange chromatography using the UPLC system and visualized by compound 1 fluorescence. (D) Graph showing total (filled bars) and tetrameric (open bars) $^{FT}TTR^{WT}$ in conditioned media prepared in the presence of Taf-S on HEK293T cells treated for 16 h with Tg (500 nM) and/or ISRB (200 nM). Total and tetrameric $^{FT}TTR^{WT}$ are normalized to media prepared on vehicle-treated cells. Relative populations of non-native TTR in each condition are shown. Error bars show SEM for $n = 10$ independent experiments. (E) Representative chromatogram showing $^{FT}TTR^{WT}$ tetramers in conditioned media prepared in the presence of Taf-S on HEK293T cells treated for 16 h with Tg (500 nM) and/or ISRB (200 nM). $^{FT}TTR^{WT}$ tetramers were separated on anion exchange chromatography using the UPLC system and visualized by compound 1 fluorescence. (F) Graph showing normalized $^{FT}TTR^{WT}$ tetramers in conditioned media prepared in the presence of Taf-S on HEK293T cells treated for 16 h with Tg (500 nM), ISRB (200 nM), and/or GSK (300 nM). Normalized TTR tetramers were calculated using the formula: normalized TTR tetramers for a given condition = (TTR tetramer signal condition/TTR tetramer signal veh)/(total TTR signal condition/TTR tetramer signal veh). Error bars show SEM for $n = 10$. * $p < 0.05$; ** $p < 0.01$; *** $p < 0.005$ for two-tailed paired t-test.

communication and immunological signaling. Thus, our demonstration that reduction in PERK activity can impact the conformation of secreted TTR reveals a new mechanism that could contribute to the pathogenesis of diseases associated with genetic or aging-related reductions in PERK activity. Furthermore, our results

reveal a new consideration when employing PERK inhibitors to attenuate chronic PERK activation in disease, as this approach could promote imbalances in extracellular proteostasis and function that could be detrimental for long-term organismal survival.

Materials and Methods

Plasmids, Antibodies and Reagents. The ^{FT}TTR^{A25T} and ^{FT}TTR^{WT} plasmids were prepared in the pcDNAI vector as previously reported³⁸. Antibodies were purchased from commercial sources: anti-ERdj3/DNAJB11 (Proteintech Group; Cat #15484-1-AP), anti-KDEL [10C3] (ENZO; Cat #ADI-SPA827-F), anti-HYOU1/ORP150 [C2C3] (Genetex; Cat#GTX102255), anti-TTR (Agilent; Cat #A000202-2), and anti-Flag M2 (Sigma Aldrich, Cat #F1804). Secondary antibodies for immunoblotting including IRDye Goat anti-mouse 800CW and IRDye Goat anti-rabbit 680CW were purchased from LICOR. Anti-FLAG immunopurifications were performed using anti-Flag M1 Agarose Affinity Gel (Sigma Aldrich; A4596). Tafamidis (Taf), Tafamidis-sulfonate (Taf-S), and compound 1 were generously gifted by Jeffery Kelly at TSRI. DMEM (Cat # 15-017-CM) was purchased from Cellgro. Penicillin/streptomycin (Cat# 15140122) glutamine (Cat# 25030081), and 0.25% Trypsin/EDTA (Cat# 25200056) were purchased from Invitrogen. Fetal Bovine Serum was purchased from Hyclone (Cat# 30396.03; Lot# AB10136011). Thapsigargin was purchased from Fisher Scientific (Cat #50-464-295). ISRB (Cat #SML0843) was purchased from Sigma. GSK2656157 (Cat# 9466) was purchased from BioVision.

Cell Culture, Plasmids, Transfections, and Lysates. HEK293T cells were cultured in DMEM supplemented 10% FBS, Penicillin/Streptomycin and glutamine. Cells were transfected with ^{FT}TTR^{A25T}/^{FT}TTR^{WT} in pcDNAI using calcium phosphate transfection, as previously reported³⁸. Cells were incubated in transfection media overnight and media was replaced with fresh supplemented complete media the next morning. Cells were lysed with 20 mM HEPES pH 7.2, 100 mM NaCl, 1% Triton X-100, 1 mM EDTA unless otherwise stated. Cell lysates were normalized to over all protein concentration in each sample using a Bradford assay.

[³⁵S] metabolic labeling assay. Metabolic labeling assays were performed as previously described^{37,38}. Briefly, HEK293T cells transfected with ^{FT}TTR^{A25T} pretreated for 16 h with the indicated condition were labelled for 30 min with EasyTag Express [³⁵S] Protein Labeling Mix (0.1 mCi/mL; Perkin Elmer) in DMEM lacking both Cys and Met (Invitrogen) supplemented with 10% dialyzed FBS, penicillin/streptomycin, and glutamine. Cells were then washed and incubated in complete media. At the indicated time, media and lysates were collected. ^{FT}TTR^{A25T} was then immunopurified from the lysate and media using anti-Flag M1 Agarose Affinity Gel (Sigma Aldrich) and incubated overnight. We then washed the beads and eluted ^{FT}TTR^{A25T} by boiling the beads in 3x Laemmli buffer including 100 mM DTT. Proteins were separated on a 12% SDS-PAGE gel, dried, exposed to phosphorimager plates (GE Healthcare), and imaged with a Typhoon imager. Band intensities were quantified by densitometry using ImageQuant. Fraction secreted was calculated using the equation: fraction secreted = [³⁵S]-TTR signal in media at t/[³⁵S]-TTR signal in media at t = 0 h + [³⁵S]-TTR signal in lysate at t = 0 h). Fraction remaining was calculated using the equation: fraction remaining = ([³⁵S]-TTR signal in media at t + [³⁵S]-TTR signal in lysate at t)/([³⁵S]-TTR signal in media at t = 0 h + [³⁵S]-TTR signal in lysate at t = 0 h). Fraction lysate was calculated using the equation: fraction lysate = [³⁵S]-TTR signal in lysate at t/[³⁵S]-TTR signal in media at t = 0 h + [³⁵S]-TTR signal in lysate at t = 0 h).

Media Conditioning, SDS-PAGE, CN-PAGE and Immunoblotting. HEK293T cells transfected with ^{FT}TTR^{A25T}/^{FT}TTR^{WT} were incubated overnight. The following morning media was changed and cells were incubated for 1 hour. Cells were then replated into a poly-D-lysine coated 6-well plate. The next evening, cells were treated with the indicated treatment for 16 hours and conditioned in 1 mL of media. Conditioned media was then collected and cleared from large debris by centrifugation at 1000 × g for 10 min. For SDS-PAGE, samples were boiled in Lammeli Buffer containing 100 mM DTT for 5 minutes and resolved on a 12% acrylamide gel. Gels were transferred to 0.2 μm nitrocellulose membranes at 100 V for 60 minutes. For CN-PAGE, samples were added to 5x Clear Native Page Buffer (final concentration: 0.1% Ponceau Red, 10% glycerol, 50 mM 6-aminohexanoic acid, 10 mM Bis-Tris pH 7.0) and resolved at 4 °C on a Novex NativePage 4–16% Bis-Tris Protein Gel run at 150 V for 3 hours. Protein was transferred at 100 V for 90 minutes to a 0.2 μm nitrocellulose membrane. Membranes were incubated with the indicated primary antibody overnight and then incubated with the appropriate LICOR secondary antibody. Protein bands were then visualized and quantified using the LICOR Odyssey Infrared Imaging System.

Quantification of ^{FT}TTR tetramers in conditioned media. ^{FT}TTR tetramers in conditioned media were quantified as previously described³³. Briefly, conditioned media was prepared on HEK293T cells expressing the indicated ^{FT}TTR variant treated with the indicated conditions. Conditioned media was then incubated with 5 μM compound 1 overnight. Media samples (60 μL) were separated over a Waters Protein-Pak Hi Res Q, 5 μm 4.6 × 100 mm anion exchange column in 25 mM Tris pH 8.0, 1 mM EDTA with a linear 1 M NaCl gradient using a ACQUITY UPLC H-Class Bio System (Waters). Fluorescence of TTR tetramers conjugated to compound 1 was observed by excitation at 328 nm and emission at 430 nm. Peaks were integrated and data was collected using Empower 3 software according to the manufacturer's protocol.

Liquid chromatography (LC)-mass spectrometry of immunopurified ^{FT}TTR. Media was conditioned for 18 h on HEK293T cells transfected with ^{FT}TTR^{A25T} treated with the indicated condition. Media was then collected and cleared from debris by centrifugation at 1000x for 10 min. ^{FT}TTR^{A25T} was immunopurified from the conditioned media using anti-Flag M1 Agarose gel. Beads were then washed 3x with 10 mM Tris pH 8.0 100 mM NaCL containing 0.05% saponin and 2x with 10 mM Tris pH 8.0 100 mM NaCL. ^{FT}TTR^{A25T} was then eluted at 4 degrees C overnight with 50 μL of 0.1 M triethylamine pH 11.5 with gentle shaking. Eluted TTR

molecular weights were analyzed by LC-MS, as previously described³³. Briefly, eluates were separated over a 5 µm ID 300 A pore size C8 reverse-phase HPLC column (Agilent) using a 15%/min linear acetonitrile gradient and then analyzed on an 1100 MSD SL mass spectrometer (Agilent). Modified and unmodified ^{FT}TTR^{A25T} was defined by the presence of different previously reported mass shifts³³ relative to the parent mass. The absolute abundance of each modified ^{FT}TTR^{A25T} peak was defined for each sample then divided by the total abundance of ^{FT}TTR^{A25T} to define the reported percent abundance for each species.

Statistical Methods. All p-values were calculated using a paired student's t-test.

References

- Ma, K., Vattem, K. M. & Wek, R. C. Dimerization and release of molecular chaperone inhibition facilitate activation of eukaryotic initiation factor-2 kinase in response to endoplasmic reticulum stress. *J Biol Chem* **277**, 18728–18735, <https://doi.org/10.1074/jbc.M200903200> (2002).
- Harding, H. P., Zhang, Y. & Ron, D. Protein translation and folding are coupled by an endoplasmic-reticulum-resident kinase. *Nature* **397**, 271–274, <https://doi.org/10.1038/16729> (1999).
- Harding, H. P. et al. Regulated translation initiation controls stress-induced gene expression in mammalian cells. *Mol Cell* **6**, 1099–1108 (2000).
- Vattem, K. M. & Wek, R. C. Reinitiation involving upstream ORFs regulates ATF4 mRNA translation in mammalian cells. *Proc Natl Acad Sci USA* **101**, 11269–11274, <https://doi.org/10.1073/pnas.0400541101> (2004).
- Lu, P. D., Harding, H. P. & Ron, D. Translation reinitiation at alternative open reading frames regulates gene expression in an integrated stress response. *J Cell Biol* **167**, 27–33, <https://doi.org/10.1083/jcb.200408003> (2004).
- Ma, Y. & Hendershot, L. M. Delineation of a negative feedback regulatory loop that controls protein translation during endoplasmic reticulum stress. *J Biol Chem* **278**, 34864–34873, <https://doi.org/10.1074/jbc.M301107200> (2003).
- Novoa, I., Zeng, H., Harding, H. P. & Ron, D. Feedback inhibition of the unfolded protein response by GADD34-mediated dephosphorylation of eIF2alpha. *J Cell Biol* **153**, 1011–1022 (2001).
- Cullinan, S. B. & Diehl, J. A. PERK-dependent activation of Nrf2 contributes to redox homeostasis and cell survival following endoplasmic reticulum stress. *J Biol Chem* **279**, 20108–20117, <https://doi.org/10.1074/jbc.M314219200> (2004).
- Cullinan, S. B. et al. Nrf2 is a direct PERK substrate and effector of PERK-dependent cell survival. *Mol Cell Biol* **23**, 7198–7209 (2003).
- Harding, H. P. et al. An integrated stress response regulates amino acid metabolism and resistance to oxidative stress. *Mol Cell* **11**, 619–633 (2003).
- Lebeau, J. et al. The PERK Arm of the Unfolded Protein Response Regulates Mitochondrial Morphology during Acute Endoplasmic Reticulum Stress. *Cell Rep* **22**, 2827–2836, <https://doi.org/10.1016/j.celrep.2018.02.055> (2018).
- Rainbolt, T. K., Atanassova, N., Genereux, J. C. & Wiseman, R. L. Stress-regulated translational attenuation adapts mitochondrial protein import through Tim17A degradation. *Cell Metab* **18**, 908–919, <https://doi.org/10.1016/j.cmet.2013.11.006> (2013).
- McQuiston, A. & Diehl, J. A. Recent insights into PERK-dependent signaling from the stressed endoplasmic reticulum. *F1000Res* **6**, 1897, <https://doi.org/10.12688/f1000research.12138.1> (2017).
- Hetz, C. & Papa, F. R. The Unfolded Protein Response and Cell Fate Control. *Mol Cell* **69**, 169–181, <https://doi.org/10.1016/j.molcel.2017.06.017> (2018).
- Hughes, D. & Mallucci, G. R. The unfolded protein response in neurodegenerative disorders - therapeutic modulation of the PERK pathway. *FEBS J*, <https://doi.org/10.1111/febs.14422> (2018).
- Hetz, C. & Saxena, S. ER stress and the unfolded protein response in neurodegeneration. *Nat Rev Neurosci* **13**, 477–491, <https://doi.org/10.1038/nrnuro.2017.99> (2017).
- Delepine, M. et al. EIF2AK3, encoding translation initiation factor 2-alpha kinase 3, is mutated in patients with Wolcott-Rallison syndrome. *Nat Genet* **25**, 406–409, <https://doi.org/10.1038/78085> (2000).
- Harding, H. P. et al. Diabetes mellitus and exocrine pancreatic dysfunction in perk-/- mice reveals a role for translational control in secretory cell survival. *Mol Cell* **7**, 1153–1163 (2001).
- Yuan, S. H. et al. Tauopathy-Associated PERK Alleles are Functional Hypomorphs that Increase Neuronal Vulnerability to ER Stress. *Hum Mol Genet*, <https://doi.org/10.1093/hmg/ddy297> (2018).
- Hoglinger, G. U. et al. Identification of common variants influencing risk of the tauopathy progressive supranuclear palsy. *Nat Genet* **43**, 699–705, <https://doi.org/10.1038/ng.859> (2011).
- Bruch, J. et al. PERK activation mitigates tau pathology *in vitro* and *in vivo*. *EMBO Mol Med* **9**, 371–384, <https://doi.org/10.15252/emmm.201606664> (2017).
- Jerry Chiang, W. C. & Lin, J. H. The effects of IRE1, ATF6, and PERK signaling on adRP-linked rhodopsins. *Adv Exp Med Biol* **801**, 661–667, https://doi.org/10.1007/978-1-4614-3209-8_83 (2014).
- Chiang, W. C., Hiramatsu, N., Messah, C., Kroeger, H. & Lin, J. H. Selective activation of ATF6 and PERK endoplasmic reticulum stress signaling pathways prevent mutant rhodopsin accumulation. *Invest Ophthalmol Vis Sci* **53**, 7159–7166, <https://doi.org/10.1167/iovs.12-10222> (2012).
- Shi, Y. et al. Identification and characterization of pancreatic eukaryotic initiation factor 2 alpha-subunit kinase, PEK, involved in translational control. *Mol Cell Biol* **18**, 7499–7509 (1998).
- Gupta, S., McGrath, B. & Cavener, D. R. PERK (EIF2AK3) regulates proinsulin trafficking and quality control in the secretory pathway. *Diabetes* **59**, 1937–1947, <https://doi.org/10.2337/db09-1064> (2010).
- Kondratyev, M., Avezov, E., Shenkman, M., Groisman, B. & Lederkremer, G. Z. PERK-dependent compartmentalization of ERAD and unfolded protein response machineries during ER stress. *Exp Cell Res* **313**, 3395–3407, <https://doi.org/10.1016/j.yexcr.2007.07.006> (2007).
- Brodsky, J. L. Cleaning up: ER-associated degradation to the rescue. *Cell* **151**, 1163–1167, <https://doi.org/10.1016/j.cell.2012.11.012> (2012).
- Hisanaga, S. et al. PERK-mediated translational control is required for collagen secretion in chondrocytes. *Sci Rep* **8**, 773, <https://doi.org/10.1038/s41598-017-19052-9> (2018).
- Sowers, C. R. et al. The protein kinase PERK/EIF2AK3 regulates proinsulin processing not via protein synthesis but by controlling endoplasmic reticulum chaperones. *J Biol Chem* **293**, 5134–5149, <https://doi.org/10.1074/jbc.M117.813790> (2018).
- Harding, H. P., Zyryanova, A. F. & Ron, D. Uncoupling proteostasis and development *in vitro* with a small molecule inhibitor of the pancreatic endoplasmic reticulum kinase, PERK. *J Biol Chem* **287**, 44338–44344, <https://doi.org/10.1074/jbc.M112.428987> (2012).
- Athanasiou, D. et al. The role of the ER stress-response protein PERK in rhodopsin retinitis pigmentosa. *Hum Mol Genet* **26**, 4896–4905, <https://doi.org/10.1093/hmg/ddx370> (2017).
- Genereux, J. C. et al. Unfolded protein response-induced ERdj3 secretion links ER stress to extracellular proteostasis. *EMBO J* **34**, 4–19, <https://doi.org/10.15252/embj.201488896> (2015).
- Chen, J. J. et al. Endoplasmic Reticulum Proteostasis Influences the Oligomeric State of an Amyloidogenic Protein Secreted from Mammalian Cells. *Cell Chem Biol* **23**, 1282–1293, <https://doi.org/10.1016/j.chembiol.2016.09.001> (2016).

34. Chen, K. C. *et al.* The endoplasmic reticulum HSP40 co-chaperone ERdj3/DNAJB11 assembles and functions as a tetramer. *EMBO J* **36**, 2296–2309, <https://doi.org/10.1525/embj.201695616> (2017).
35. Eisele, Y. S. *et al.* Targeting protein aggregation for the treatment of degenerative diseases. *Nat Rev Drug Discov* **14**, 759–780, <https://doi.org/10.1038/nrd4593> (2015).
36. Sekijima, Y. Transthyretin (ATTR) amyloidosis: clinical spectrum, molecular pathogenesis and disease-modifying treatments. *J Neurol Neurosurg Psychiatry* **86**, 1036–1043, <https://doi.org/10.1136/jnnp-2014-308724> (2015).
37. Chen, J. J. *et al.* ATF6 activation reduces the secretion and extracellular aggregation of destabilized variants of an amyloidogenic protein. *Chem Biol* **21**, 1564–1574, <https://doi.org/10.1016/j.chembiol.2014.09.009> (2014).
38. Shoulders, M. D. *et al.* Stress-independent activation of XBP1s and/or ATF6 reveals three functionally diverse ER proteostasis environments. *Cell Rep* **3**, 1279–1292, <https://doi.org/10.1016/j.celrep.2013.03.024> (2013).
39. Sidrauski, C. *et al.* Pharmacological brake-release of mRNA translation enhances cognitive memory. *eLife* **2**, e00498, <https://doi.org/10.7554/eLife.00498> (2013).
40. Sidrauski, C. *et al.* Pharmacological dimerization and activation of the exchange factor eIF2B antagonizes the integrated stress response. *eLife* **4**, e07314, <https://doi.org/10.7554/eLife.07314> (2015).
41. Axtell, J. M. *et al.* Discovery of GSK2656157: An Optimized PERK Inhibitor Selected for Preclinical Development. *ACS Med Chem Lett* **4**, 964–968, <https://doi.org/10.1021/ml400228e> (2013).
42. Rojas-Rivera, D. *et al.* When PERK inhibitors turn out to be new potent RIPK1 inhibitors: critical issues on the specificity and use of GSK2606414 and GSK2656157. *Cell Death Differ* **24**, 1100–1110, <https://doi.org/10.1038/cdd.2017.58> (2017).
43. Choi, S., Ong, D. S. & Kelly, J. W. A stilbene that binds selectively to transthyretin in cells and remains dark until it undergoes a chemoselective reaction to create a bright blue fluorescent conjugate. *J Am Chem Soc* **132**, 16043–16051, <https://doi.org/10.1021/ja104999y> (2010).
44. Rappley, I. *et al.* Quantification of transthyretin kinetic stability in human plasma using subunit exchange. *Biochemistry* **53**, 1993–2006, <https://doi.org/10.1021/bi500171j> (2014).
45. Sekijima, Y. *et al.* The biological and chemical basis for tissue-selective amyloid disease. *Cell* **121**, 73–85, <https://doi.org/10.1016/j.cell.2005.01.018> (2005).

Acknowledgements

We thank Evan Powers, Bibiana Rius, and Jessica Rosarda for critical reading of this manuscript. We thank Jeff Kelly (TSRI) for access to the UPLC instrument and compound **1**, Taf, and Taf-S. This work was funded by NIH NS092829 to RLW.

Author Contributions

I.C.R. and R.L.W. conceived of the experiments, performed the experiments, analyzed the results, and wrote the manuscript.

Additional Information

Supplementary information accompanies this paper at <https://doi.org/10.1038/s41598-018-37207-0>.

Competing Interests: The authors declare no competing interests.

Publisher's note: Springer Nature remains neutral with regard to jurisdictional claims in published maps and institutional affiliations.



Open Access This article is licensed under a Creative Commons Attribution 4.0 International License, which permits use, sharing, adaptation, distribution and reproduction in any medium or format, as long as you give appropriate credit to the original author(s) and the source, provide a link to the Creative Commons license, and indicate if changes were made. The images or other third party material in this article are included in the article's Creative Commons license, unless indicated otherwise in a credit line to the material. If material is not included in the article's Creative Commons license and your intended use is not permitted by statutory regulation or exceeds the permitted use, you will need to obtain permission directly from the copyright holder. To view a copy of this license, visit <http://creativecommons.org/licenses/by/4.0/>.

© The Author(s) 2019